J Incl Phenom Macrocycl Chem (2011) 71:455–462
DOI 10.1007/s10847-011-0007-6

ORIGINAL ARTICLE

New metal organic frameworks incorporating the ditopic macrocyclic ligand dipyridyldibenzotetraaza[14]annulene

Yanyan Mulyana · Leonard F. Lindoy · Cameron J. Kepert · John McMurtrie · Andrew Parkin · Peter Turner · Gang Wei · J. G. Wilson

Received: 26 May 2011 / Accepted: 19 June 2011 / Published online: 19 July 2011

Abstract The synthesis and crystal structures of three new metal organic frameworks of type $[Zn(\mathbf{L}\text{-}2H)]_n$ (**1**), $\{[Zn\mathbf{L}Cl_2](CH_3CN)_{0.5}(DMF)_{0.5}(H_2O)_{0.5}\}_n$ (**2**) and $\{[Cd\mathbf{L}(DMF)(NO_3)_2]\cdot DMF\}_n$ (**3**), all based on the dipyridyl-derivatised macrocycle, dipyridyldibenzotetraaza[14]annulene (**L**), are reported along with the X-ray structure of the protonated metal-free ligand as its perchlorate salt, $[(H\mathbf{L})(ClO_4)]_n$ (**4**). In $[Zn(\mathbf{L}\text{-}2H)]_n$, the zinc ion occupies the macrocyclic cavity, being bound to the N_4-donor set of the macrocyclic ring in its doubly deprotonated form. Each zinc atom is also axially bound by a pyridyl moiety from an adjacent complex, resulting in formation of an infinite one-dimensional chain of the 'herringbone' type in which pairs of macrocyclic complexes interact via face-to-face π–π stacking interactions. In contrast, the zinc ion in $\{[Zn\mathbf{L}Cl_2](CH_3CN)_{0.5}(DMF)_{0.5}(H_2O)_{0.5}\}_n$ does not occupy the macrocyclic cavity but is bound to a pyridyl nitrogen from two ligands such that it acts as a bridge between macrocyclic units and results in the generation of a one-dimensional chain. Two chloro ligands also bind to each zinc centre to yield a distorted tetrahedral coordination geometry. Offset π–π stacking occurs between adjacent chains involving alternate macrocycles in each chain, giving rise to a zig-zag arrangement. Pairs of interacting chains pass through the above-mentioned chains to generate further π–π stacking to yield an overall three-dimensional structure that contains large ellipsoidal-shaped channels. In $\{[Cd\mathbf{L}(DMF)(NO_3)_2]\cdot DMF\}_n$ the cadmium ion again does not occupy the macrocyclic cavity but acts as a bridge between macrocycles to once again afford a linear chain structure. Each cadmium is bound to two pyridyl groups (arising from different molecules of **L**), two nitrato ligands and one oxygen-bound dimethylformamide molecule to yield a distorted pentagonal bipyramidal coordination geometry. The protonated ligand, $[(H\mathbf{L})(ClO_4)]_n$, adopts a linear chain structure in which one pyridyl group is protonated and interacts intermolecularly via a hydrogen bond with the non-protonated pyridyl group of an adjacent macrocyclic unit to yield a hydrogen-bonded linear chain structure.

Keywords Macrocycle · Zinc(II) · Cadmium(II) · Coordination polymer · X-ray · Dibenzotetraaza[14]annulene

Andrew Parkin—deceased.
Y. Mulyana, C. J. Kepert, J. McMurtrie, P. Turner, G. Wei and J. G. Wilson dedicate this manuscript to Prof. Len Lindoy in celebration of his 75th birthday.

Y. Mulyana · L. F. Lindoy · C. J. Kepert · P. Turner · J. G. Wilson
School of Chemistry, University of Sydney, Sydney NSW 2006, Australia
e-mail: yanyan.mulyana@jcu.edu.au

J. McMurtrie (✉)
Department of Chemistry, Faculty of Science and Technology, Queensland University of Technology, GPO Box 2434, Brisbane QLD 4001, Australia
e-mail: j.mcmurtrie@qut.edu.au

A. Parkin
Department of Chemistry, University of Glasgow, University Avenue, Glasgow G12 8QQ, UK

G. Wei
CSIRO Materials Science and Engineering, P.O. Box 218, Lindfield NSW 2070, Australia

Introduction

The increased interest in molecular frameworks over the past decade or so has been reflected by the synthesis of a large

number of polymeric structures that range from linear chains to multi-connected arrays [1–10]. In part, such studies have been driven by the prospect of obtaining new materials that might find application in a number of areas [11–13], including catalysis, sensing, light-harvesting devices and opto-electronics. While a very considerable number of studies have involved extended arrays incorporating 4,4′-bipyridyl and related ligands [14], only a limited number of systems of this type have incorporated macrocyclic spacer groups [15]. The latter include metallo frameworks incorporating tetrapyridylporphyrin (tpp); for example, a structure in which palladium(II)-metallated tpp units were interconnected by cadmium(II) ions has been reported [16] along with the use of tpp for the synthesis of framework materials incorporating copper(I) [17], cobalt(II) [18], manganese(II) [18], mercury(II) [19, 20], lead(II) [20], cadmium(II) [20] as well as metal oxides [21]. We now report the synthesis and structures of three new linear frameworks of this general type incorporating the synthetic ditopic macrocycle,

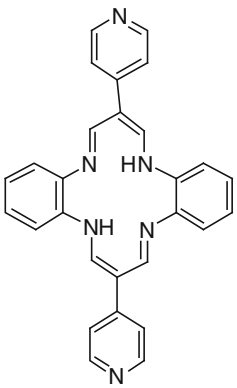

L

dipyridyldibenzotetraaza[14]annulene (**L**), together with one structure in which molecules of **L** are linked by hydrogen bonds.

Experimental

Where available, all chemicals were of analytical grade and were used without further purification. Macrocycle **L** was prepared using the literature procedure [22]. All products were dried over silica gel before microanalysis. Crystals used for the X-ray studies were removed from the mother liquor and used directly for the structure determinations.

Framework synthesis

$[Zn(L\text{-}2H]_n$ (1)

A mixture of **L** (0.05 mmol) and zinc(II) chloride (0.1 mmol) in dimethylformamide (10 mL) was placed in a Teflon-sealed bomb and heated to 155 °C over 5 h. The system was maintained isothermally for 10 h and then let cool to room temperature over 60 h. Dark red plate-like crystals were obtained. Calc. for $C_{28}H_{20}N_6Zn$: C, 66.48; H, 3.98; N, 16.61. Found: C, 66.18; H, 4.07; N, 16.68%.

$\{[ZnLCl_2]\cdot(CH_3CN)_{0.5}(DMF)_{0.5}(H_2O)_{0.5}\}_n$ (2)

To a stirred solution of **L** (0.05 mmol) in dimethylformamide (5 mL) was added zinc(II) chloride (0.1 mmol) in acetonitrile (2 mL) at room temperature. Red prismatic crystals grew over several days. Calc. for $C_{28}H_{22}N_6ZnCl_2\cdot 2.5H_2O$: C, 53.91; H, 4.36; N, 13.47. Found: C, 53.59; H, 4.01; N, 13.62%.

$\{[CdL(DMF)(NO_3)_2]\cdot DMF\}_n$ (3)

To **L** (0.05 mmol) in dimethylformamide (5 mL) was added cadmium(II) nitrate (0.1 mmol, 2 mL) in methanol (2 mL). Red columnar crystals grew over several weeks. Calc. for $C_{28}H_{22}N_8O_6Cd\cdot C_2H_6OS$: C, 49.49; H, 4.40; N, 16.98. Found: C, 49.09; H, 4.59; N, 16.89%.

$\{[(HL)(ClO_4)]\}_n$ (4)

The preparation of this ligand salt was carried out in a H-shaped tube. A solution of **L** (0.05 mmol) in benzyl alcohol (1 mL) was placed in one arm of a H-shaped tube. In the second arm was placed a solution of iron(II) perchlorate (0.5 mmol) and ammonium thiocyanate (1 mmol) in ethanol (1 mL). A mixture of benzyl alcohol and ethanol (2:1) was carefully layered over both reagent solutions to connect both halves of the tube which was then stoppered and let stand. Crystals that were free of thiocyanate grew over a period of several weeks.

X-ray structure determinations

Single crystal X-ray diffraction data for the structure determinations were collected on a Bruker-AXS SMART 1000 CCD diffractometer equipped with an Oxford Cryosystems Cryostream nitrogen gas stream and an Oxford Cryosystems helium gas stream. Single crystals were quench-cooled to 150 K under a nitrogen gas stream and diffraction patterns were obtained using graphite monochromated Mo Kα radiation. Data integration and reduction were undertaken with SAINT and XPREP [23], and subsequent computations were carried out using the teXsan [24], WinGX-32, [25] and XTAL [26] graphical user interfaces. A Gaussian absorption correction was applied to the data for **1** and **3**, no absorption correction was applied for **2** and an empirical absorption correction determined with

SADABS [27] was used for **4**. All structures were solved by direct methods (using SIR97 [28] for **1**–**3** and SHELXS-97 [29] for **4**) and extended and refined with SHELXL-Plus [30]. For **1** and **3**, all non-hydrogen atoms were modelled with anisotropic displacement parameters. A riding atom model with group displacement parameters was used for all hydrogen atoms in **1**, and for hydrogen atoms attached to carbon atoms in **3**. H(1 N) and H(3 N) attached to nitrogen atoms N(1) and N(3) in **3** were located on the difference map and their coordinates were refined with idealised bond length restraints. The thermal parameters for atoms H(1 N) and H(3 N) were fixed, riding at 1.2 times the Ueq of the attached nitrogen atoms. Complex **2** proved to be a non-merohedral twin. The data set was treated with the program Gemini [31] in an attempt to index the separate twin components and allow integration of the data with respect to each. This did not lead to an acceptable result due to significant overlapping of a large proportion of the reflections from the twin components. Partial data sets were collected using several different crystals in an attempt to find a more suitable crystal for structure determination; however, all these displayed non-merohedral twinning. Consequently, structure solution and refinement was carried out using data from the first collection with indexing only on the principle twin fraction. The difference Fourier map displayed regions of smeared electron density typically associated with the presence of disordered solvent molecules. A model incorporating one dimethylformamide (DMF) molecule (disordered over four sites), one acetonitrile molecule (disordered over four sites) and one water molecule (disordered over five sites) was employed in an attempt to describe the disordered solvent. In the crystal lattice the disordered solvent occupies large continuous channels that run parallel to the crystallographic *a* axis. Dimethylformamide and acetonitrile molecules were refined as rigid groups. In order to achieve intramolecular consistency of thermal motion, the thermal

Table 1 Crystallographic data

Parameter	Crystals			
	1	2	3	4
Formula	$C_{56}H_{40}N_{12}Zn_2$	$C_{30.5}H_{28}N_7OCl_2$ Zn	$C_{34}H_{36}N_{10}O_8Cd$	$C_{28}H_{23}ClN_6O_4$
Mr	1011.74	644.87	*M* = 825.13	542.97
Crystal system	Monoclinic	Monoclinic	Monoclinic	Monoclinic
Space group	*P*21/*n* (#14)	*P*21/*c* (#14)	*P*21/*c* (#14)	*C*2/*c* (#15)
a/Å	8.960 (2)	14.451 (8)	21.018 (16)	52.425 (6)
b/Å	14.703 (4)	27.772 (15)	10.165 (8)	10.0020 (12)
c/Å	16.911 (5)	16.553 (9)	18.029 (14)	18.894 (3)
β/^{o}	90.232 (6)	92.220 (10)	112.799 (12)	99.948 (7)
V/Å^3	2227.8 (10)	6638 (6)	3551 (5)	9758 (2)
*D*c/g cm^{-3}	1.508	1.291	1.543	1.478
Z	2	8	4	16
Crystal size/mm	0.185 × 0.134 × 0.008	0.35 × 0.21 × 0.10	0.81 × 0.09 × 0.07	0.72 × 0.71 × 0.55
Crystal colour	Red	Red	Orange	Red
Crystal habit	Plate	Prism	Columnar	Block
Temperature/K	150 (2)	150 (2)	150 (2)	150 (2)
λ(MoKα)/Å	0.71073	0.71073	0.71073	0.71073
μ(MoKα)/mm^{-1}	1.133	0.934	0.681	0.207
T(SADABS)min, max	0.823, 0.990	Not measured	Not measured	0.842, 1.000
2*θ*max/^{o}	56.60	56.58	56.60	45.12
hkl range	−11 11, −19 19, −22 22	−19 19, −35 31, −19 21	−27 27, −13 13, −23 23	−53 55, −10 10, −15 20
N	25,484	42,889	30,740	15,693
Nind	5,517 (*R*merge, 0.0506)	15,418 (*R*merge, 0.127)	8374 (*R*merge, 0.0631)	5,701 (*R*merge, 0.0425)
Nobs	4,075 (I > 2*σ*(I))	7,690 (I > 2*σ* (I))	6338 (I > 2*σ*(I))	2,841 (I > 2*σ*(I))
Nvar	316	687	488	409
Residuals* *R*1(*F*), *wR*2(*F*2)	0.032, 0.068[a]	0.157, 0.464[a]	0.030, 0.084[a]	0.083, 0.288[a]
GoF (all)	1.200	1.441	1.092	1.024
Residual extrema/e−Å^{-3}	−0.369, 0.666	−1.621, 1.654	−0.713, 0.736	−1.250, 0.772

[a] $R1 = \Sigma||F_o|-|F_c||/\Sigma|F_o|$ for $F_o > 2\sigma(F_o)$ and $wR2 = (\Sigma w(F_o^2-F_c^2)^2/\Sigma(wF_c^2)^{1/2}$ where $w = 1/[\sigma^2(F_o^2) + (AP)^2 + BP]$, $P = (F_o^2 + 2F_c^2)/3$; $A = 0.002$, $B = 0.30$ for **1**; $A = 0.20$, $B = 0.00$ for **2**; $A = 0.00362$, $B = 0.10$ for **3**; $A = 0.1732$, $B = 2.1771$ for **4**

parameters for the atoms of disordered groups were refined isotropically with values fixed at 0.06. The occupancies of the disordered groups were refined for several refinement cycles then fixed at appropriate and internally consistent values for the final refinement cycles. Least squares convergence was only obtainable by applying positional restraints and/or constraints to the atoms of disordered solvent molecules. All ordered non-hydrogen atoms were refined anisotropically and a riding atom model was used for the refinement of hydrogen atoms. For **4**, all carbon atoms were modelled with isotropic displacement parameters to improve the low data:parameter ratio, and all perchlorate oxygen atoms were modelled as isotropic due to high thermal disorder. All nitrogen and chlorine atoms were refined as anisotropic. Distance restraints were applied to all chlorine–oxygen bond lengths and all oxygen–chlorine–oxygen 1,3-distances. A riding atom model with group displacement parameters was used for the hydrogen atoms. A summary of the refinement parameters is included as Table 1. The CIF files have been deposited with the Cambridge Structural Database (CCDC reference numbers 827087–827090) and can be obtained free of charge via www.ccdc.cam.ac.uk/conts/retrieving.html (or from the Cambridge Crystallographic Data Centre, 12 Union Road, Cambridge CB2 1EZ, UK; fax: (+44) 1223-336-033; or deposit@ccdc.cam.ac.uk).

Two linear frameworks incorporating zinc(II)

The employment of two synthetic procedures for interacting **L** with zinc(II) chloride led to the formation of different products. Dark red plate-like crystals (**1**) were obtained from a solvothermal synthesis in which **L** was reacted with zinc(II) chloride in dimethylformamide at 155 °C. When a solution of **L** in dimethylformamide was again treated with zinc(II) chloride in acetonitrile at ambient temperature, red block crystals (**2**) grew after several days. Microanalysis results for the two crystal types indicated that they had different elemental compositions. Based on an X-ray single crystal structural determination, the crystals corresponding to **1** were shown to be of type [Zn(**L**-2H)] whereas those for **2** correspond to a formula unit of type $[Zn\mathbf{L}Cl_2]\cdot x$ guest.

In **1**, zinc(II) coordination by the N_4-donor set of the macrocycle occurs with a pyridyl group from a second macrocyclic complex occupying the fifth coordination site such that the coordination geometry approximates a distorted square pyramid. The zinc centre is displaced from the N_4-plane by 0.51 Å towards the apical pyridyl nitrogen (Fig. 1). This arrangement creates a one dimensional polymeric chain that essentially contains no solvent-accessible voids. Each chain forms a 'herringbone' arrangement in which pairs of macrocyclic complexes

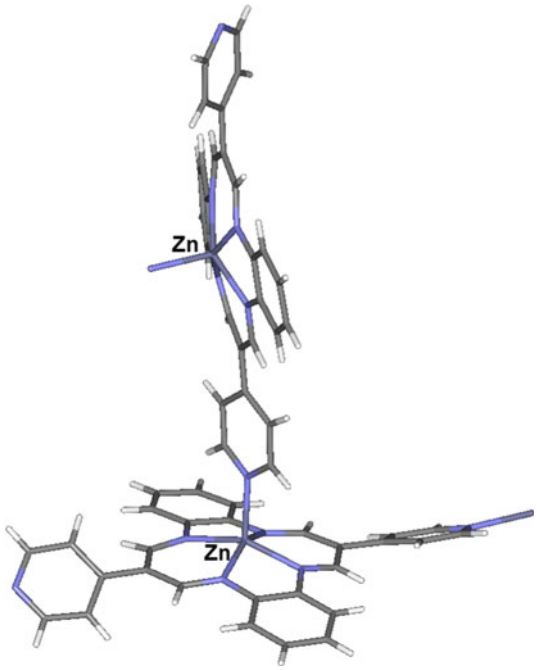

Fig. 1 The distorted square pyramidal geometry in $[Zn(\mathbf{L}\text{-}2H)]_n$

interact closely with each other via face-to-face π–π stacking interactions Fig. 2.

This coordination system creates a one dimensional polymeric chain that essentially contains no solvent-accessible voids. Each chain adopts a 'herringbone' arrangement and these interact closely with one another via face-to-face π–π stacking interactions.

In contrast to the above structure, the crystal structure of $\{[Zn\mathbf{L}Cl_2](CH_3CN)_{0.5}(DMF)_{0.5}(H_2O)_{0.5}\}_n$ (**2**) shows that the zinc(II) ion does not occupy the macrocyclic cavity. The asymmetric unit (Fig. 3) contains a coordinate polymer fragment incorporating two molecules of **L** bound via pyridyl nitrogen atoms to two zinc(II) atoms. Each zinc(II) atom is also bound to two chlorine atoms which provide charge balance. The N(5)–Zn(1)–N(12) bond angle, at 107.3(4)°, is close to the ideal tetrahedral value while the N–Zn(1)–Cl angles range from 103.5(3)° to 107.1(3)°. The major distortion of the tetrahedral centre is observed for the Cl(3)–Zn(2)–Cl(4) bond angle which is significantly larger than ideal at 124.43(16)°. A search of the CSD showed that Cl–Zn–Cl bond angles for the $Zn(py)_2Cl_2$ fragment with approximate tetrahedral stereochemistry (32 structures) vary between 110° and 130° (mean 119, SD 4.08) in accord with the geometry of the zinc(II) centre in the present structure being unexceptional; similarly, the respective Zn–N and Zn–Cl bond lengths are also with normal limits for such bonds.

There is offset π–π stacking between chains that involves alternate macrocycles in each chain, the latter adopting a zig-zag arrangement. Pairs of interacting chains

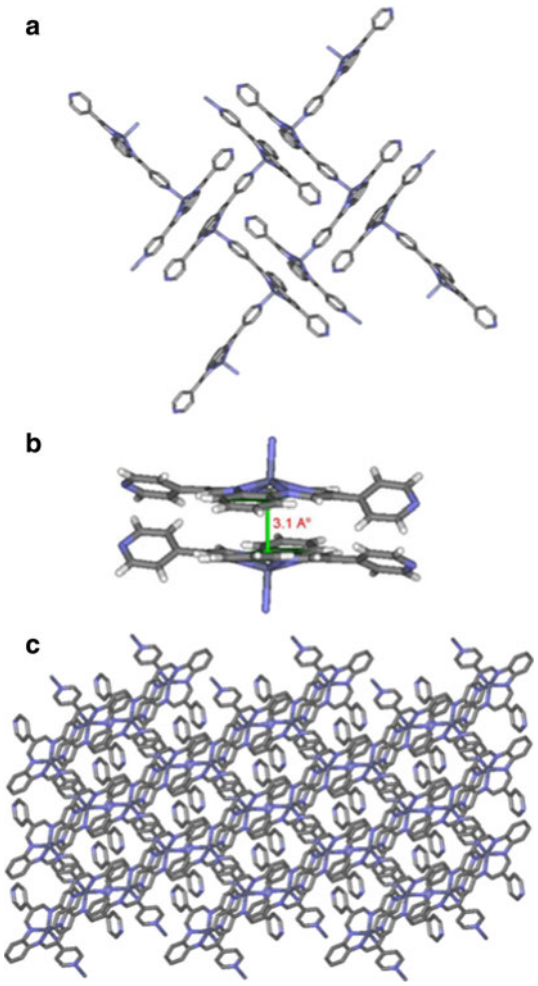

Fig. 2 **a**, **b** Interaction between the chains in a crystal of [Zn(**L**-2H)]$_n$ (**1**), showing face-to-face π–π stacking at 3.1 Å. **c** Crystal packing along the b-axis (bottom)

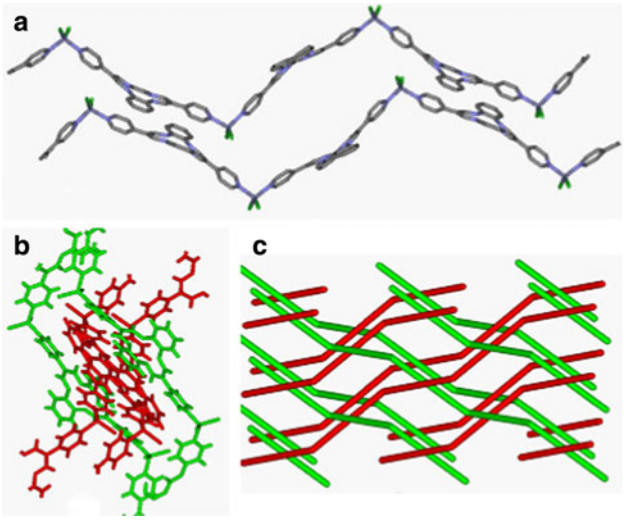

Fig. 4 **a** The one-dimensional zigzag chains in {[Zn**L**Cl$_2$]·(DMF)$_{0.5}$(CH$_3$CN)$_{0.5}$(H$_2$O)$_{0.5}$}$_n$ (**2**); offset π–π stacking of two macrocycles from adjacent chains is shown. **b** The overlaying of two pairs of the chains is shown. **c** Schematic of the alternate overlaying of the pairs of the chains that gives rise to three-dimensional connectivity

pass through the above-mentioned chains (in regions where no direct π–π stacking is present) to generate an overall three-dimensional π–π stacked structure (Fig. 4).

The above interweaving between pairs of one-dimensional chains gives rise to a framework that contains large ellipsoidal channels (Fig. 5). Disordered solvent molecules reside in the channels.

A linear framework involving cadmium(II)

Treatment of **L** with cadmium(II) nitrate in a 2:1 mixture of dimethylformamide and methanol led to the formation of red

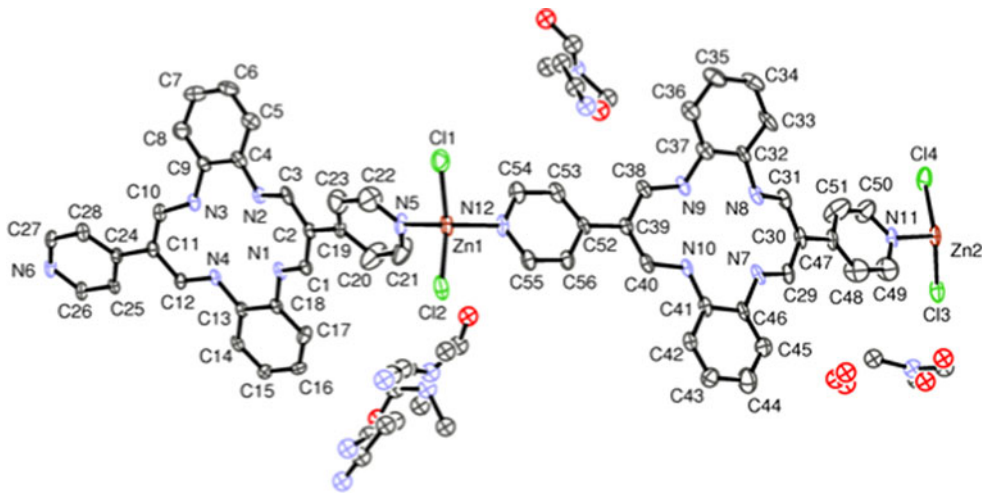

Fig. 3 An ORTEP [32] diagram of the asymmetric unit of {[Zn**L**Cl$_2$]·(DMF)$_{0.5}$(CH$_3$CN)$_{0.5}$(H$_2$O)$_{0.5}$}$_n$ (**2**) showing 30 percent probability ellipsoids

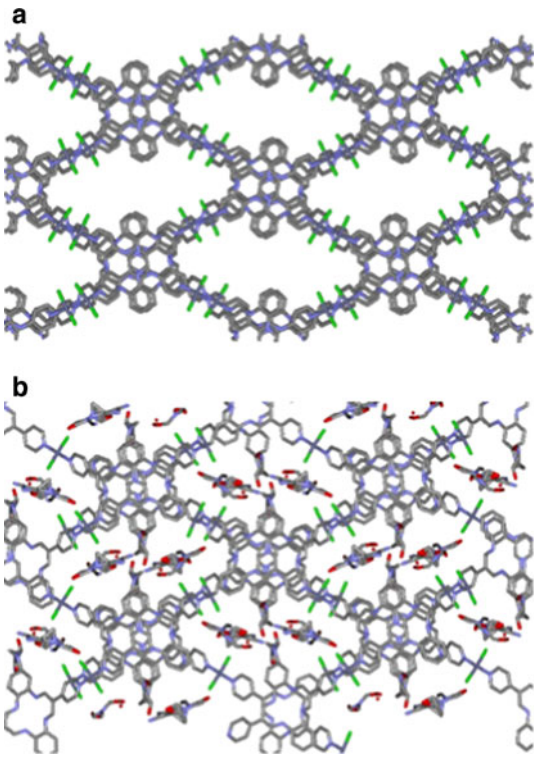

Fig. 5 **a** The three-dimensional structure of $\{[ZnLCl_2](CH_3CN)_{0.5}(DMF)_{0.5}(H_2O)_{0.5}\}_n$ (**2**) showing the solvent accessible channels. Disordered solvent molecules have been omitted. **b** View of the disordered solvent molecules residing in the channels

crystals over several weeks. An X-ray structure determination showed that the asymmetric unit corresponds to $[CdL(NO_3)_2(DMF)]\cdot DMF$ (**3**). The cadmium(II) centre is seven coordinate with an approximate pentagonal bipyramidal geometry (Fig. 6). Ligand **L** bridges adjacent cadmium(II) centres creating a 1D coordination polymeric arrangement, with the repeating unit given by $[CdL(NO_3)_2(DMF)]$. The macrocycle coordinates via its pyridyl nitrogen atoms [(N(5) to one cadmium(II) centre and N(6) to an adjacent cadmium(II) centre)] in axial positions of the respective metal bipyramidal coordination spheres. Two nitrate ligands coordinate in a bidentate fashion to each cadmium(II) in an approximate coplanar fashion such that they contribute four oxygen donors to the (approximate) pentagonal plane of each cadmium's coordination sphere. An oxygen-bound dimethylformamide molecule is also coordinated in each pentagonal plane; the second dimethylformamide molecule is present as a lattice solvate.

There is a noticeable difference in the orientation of the pyridyl terminal groups relative to the N_4-macrocyclic plane in the crystal structures of **2** and **3**. While essentially no deviation from the plane occurs in **2**, the coordinated pyridyl terminal groups in **3** both deviate to the side of the N_4-plane of the macrocycle. The resulting bent conformation results in the formation of a different π–π offset arrangement in **3** relative to that occurring in **2**.

Inspection of the positions of adjacent macrocycles in the coordination unit indicates that they are orientated approximately orthogonally with respect to each other. Overall, the structure may be considered to be essentially one dimensional (Fig. 7) with the voids occupied by dimethylformamide molecules.

Crystals of $[(HL)(ClO_4)]_n$ (**4**) were obtained on slow diffusion of **L** in benzyl alcohol into a 1:2 molar mixture of iron(II) perchlorate and ammonium thiocyanate in a H-shaped diffusion cell. Initially it was anticipated that a

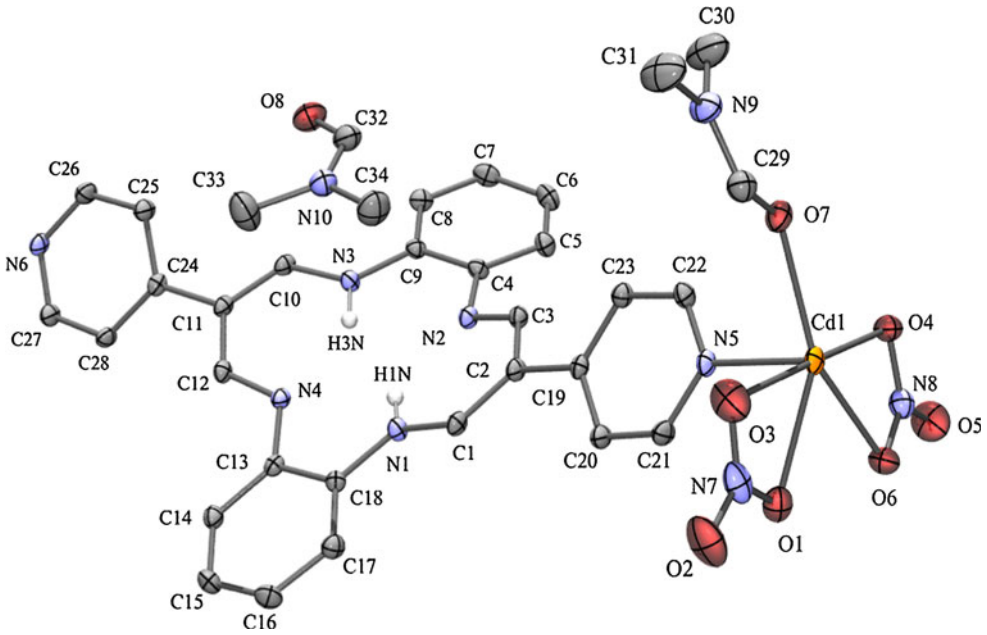

Fig. 6 ORTEP [32] plot of the asymmetric unit of $\{[CdL(NO_3)_2(DMF)]\cdot DMF\}_n$ (**3**) with displacement ellipsoids drawn at 40% probability. All hydrogen atoms except H1 N and H3 N have been omitted for clarity

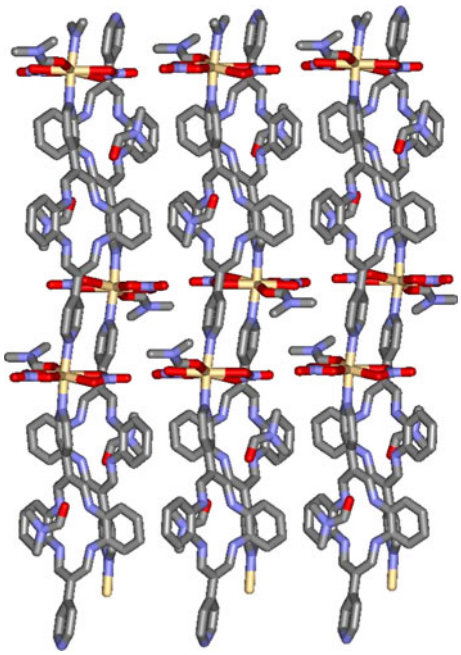

Fig. 7 View of $\{[Cd\mathbf{L}(NO_3)_2(DMF)]\cdot DMF\}_n$ (**3**) along the b-axis

framework species incorporating iron(II) complexed by **L** might form. However, under the conditions employed the product was instead the metal-free, hydrogen perchlorate salt of **L** (Fig. 8). One of the pyridyl groups in each molecule of **L** is protonated and interacts intermolecularly via a hydrogen bond to the non-protonated pyridyl group of an adjacent macrocyclic unit to yield a linear chain structure. The macrocycles in each chain are co-planar (Fig. 8) and perchlorate counterions reside nearby. There is π–π stacking between macrocycles, with the separation between rings being 3.1 Å. In this structure the two pyridyl terminal groups do not deviate from the macrocyclic N_4-donor plane.

Concluding remarks

Three new metal coordination polymers have been synthesized and their structures determined. In the case of the linear chain structure $[Zn(\mathbf{L}\text{-}2H)]_n$ (**1**), the metal ion occupies the macrocyclic cavity; this is not the case in the remaining two metal-containing structures. $\{[CdL(DMF)(NO_3)_2]\cdot DMF\}_n$ (**3**) also has a linear chain structure with the metal ion linking the macrocyclic units while $\{[ZnLCl_2](CH_3CN)_{0.5}(DMF)_{0.5}(H_2O)_{0.5}\}_n$ (**2**) has an interesting three dimensional structure based on interlinked linear strands. A metal-free, hydrogen-bonded linear polymer of type $[(H\mathbf{L})(ClO_4)]_n$ (**4**) is also reported.

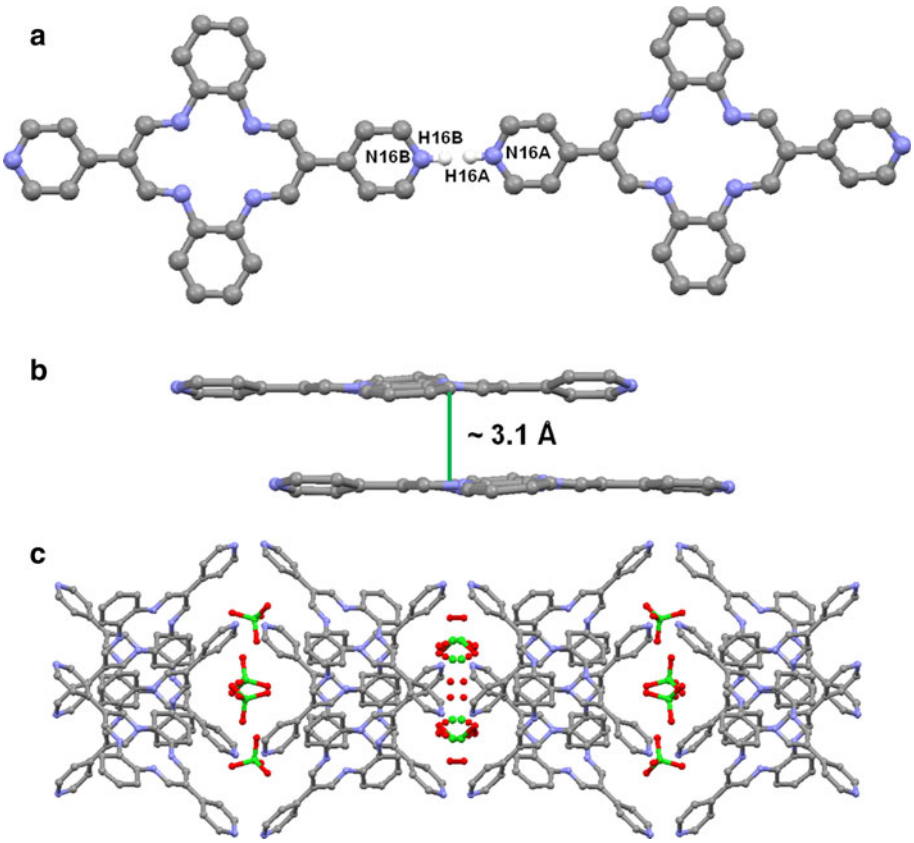

Fig. 8 **a** A hydrogen bond (1.83 Å) is formed between two pyridyl moieties [H(16A)-N(16B)] from different molecules of H**L** in $[(H\mathbf{L})(ClO_4)]_n$; the two molecules shown are crystallographically independent. Hydrogen atoms are modelled on both pyridyl nitrogen positions of the crystallographically independent molecules with 50% site occupancies. Perchlorate anions have been omitted for clarity. **b** View of the π–π offset in $[(H\mathbf{L})(ClO_4)]_n$. **c** Crystal packing along the c-axis in $[(H\mathbf{L})(ClO_4)]_n$, showing the occupancies of the perchlorate anions (some of which are disordered)

Geometric preferences of the chosen metal ions and the conformations adopted by the aromatic systems in the N_4 environment of the macrocycle have been found to be the main factors that determine the supramolecular topology of the resulting frameworks.

Acknowledgment We thank the Australian Research Council for support.

References

1. Zhang, J.-P., Huang, X.-C., Chen, X.-M.: Supramolecular isomerism in coordination polymers. Chem. Soc. Rev. **38**, 2385–2396 (2009)
2. Spokoyny, A.M., Kim, D., Sumrein, A., Mirkin, C.A.: Infinite coordination polymer nano- and microparticle structures. Chem. Soc. Rev. **38**, 1218–1227 (2009)
3. Morsali, A., Masoomi, M.Y.: Structures and properties of mercury(II) coordination polymers. Coord. Chem. Rev. **253**, 1882–1905 (2009)
4. Lin, W., Rieter, J.W., Taylor, K.M.L.: Modular synthesis of functional nanoscale coordination polymers. Angew. Chem. Int. Ed. **48**, 650–658 (2009)
5. Biradha, K., Ramanan, A., Vittal, J.J.: Coordination polymers versus metal-organic frameworks. Cryst. Growth Des. **9**, 2969–2970 (2009)
6. Murray, L.J., Dinca, M., Long, J.R.: Hydrogen storage in metal-organic frameworks. Chem. Soc. Rev. **38**, 1294–1314 (2009)
7. Robson, R.: Design and its limitations in the construction of bi- and poly-nuclear coordination complexes and coordination polymers (aka MOFs): a personal view. Dalton Trans. **38**, 5113–5131 (2008)
8. Tanaka, D., Kitagawa, S.: Template effects in porous coordination polymers. Chem. Mater. **20**, 922–931 (2008)
9. Friese, V.A., Kurth, D.G.: Soluble dynamic coordination polymers as a paradigm for materials science. Coord. Chem. Rev. **252**, 199–211 (2008)
10. Kitagawa, S., Matsuda, R.: Chemistry of coordination space of porous coordination polymers. Coord. Chem. Rev. **251**, 2490–2509 (2007)
11. Batten, S.R., Neville, S.M., Turner, D.R.: Coordination polymers: design analysis and application. RSC Publishing, Cambridge (2009)
12. Czaja, A.U., Trukhan, N., Müller, U.: Chem. Soc. Rev. **38**, 1284–1293 (2009)
13. Lee, J.-Y., Farha, O.K., Roberts, J., Scheidt, K.A., Nguyen, S.-B.T., Hupp, J.T.: Metal-organic framework materials as catalysts. Chem. Soc. Rev. **38**, 1450–1459 (2009)
14. Biradha, K., Sarkar, M., Rajput, L.: Crystal engineering of coordination polymers using 4,4′-bipyridine as a bond between transition metal atoms. Chem. Commun. **40**, 4169–4179 (2006)
15. Suh, M.P., Moon, H.R.: Coordination polymer open frameworks constructed of macrocyclic complexes. Adv. Inorg. Chem. **59**, 39–79 (2007)
16. Abrahams, B.F., Hoskins, B.F., Robson, R.: A new type of infinite 3D polymeric network containing 4-connected, peripherally-linked metalloporphyrin building blocks. J. Am. Chem. Soc. **113**, 3606–3609 (1991)
17. Abrahams, B.F., Hoskins, B.F., Michail, D.M., Robson, R.: Assembly of porphyrin building blocks into network structures with large channels. Nature **369**, 727–729 (1994)
18. Lin, K.-J.: SMTP-1: The first functionalized metalloporphyrin molecular sieves with large channels. Angew. Chem. Int. Ed. **38**, 2730 (1999)
19. Pan, L., Noll, B.C., Wang, X.: Self-assembly of free-base tetrapyridylporphyrin units by metal ion coordination. Chem. Comm. 157–158 (1999)
20. Sharma, C.V.K., Broker, G.A., Huddleston, J.G., Baldwin, J.W., Metzger, R.M., Rogers, R.D.: Design strategies for solid-state supramolecular arrays containing both mixed-metalated and freebase porphrins. J. Am. Chem. Soc. **121**, 1137 (1999)
21. Hagrman, D., Hagrman, P.J., Zubieta, J.: Solid-state coordination chemistry: the self-assembly of microporous organic-inorganic hybrid frameworks constructed from tetrapyridylporphyrin and bimetallic oxide chains or oxide clusters. Angew. Chem. Int. Ed. **38**, 3165 (1999)
22. Reichardt, C., Scheibelein, W.: Synthesis with aliphatic dialdehyde, XXVII. A non-template synthesis for the preparation of metal-free 1,4,8,11-tetraaza[14]annulene derivatives. Z. Naturforsch. **33**, 1012–1015 (1978)
23. Bruker, : SMART, SAINT and XPREP. Area detector control and data integration and reduction software. Bruker Analytical X-ray Instruments Inc, Madison (1995)
24. Molecular Structure Corporation (1997–1998). teXsan for Windows: Single structure analysis software, MSC, 3200 Research forest drive, The Woodlands, USA
25. Farrugia, L.J.: WinGX-32: system of programs for solving, refining and analysing single crystal X-ray diffraction data for small molecules. J. Appl. Cryst. **32**, 837 (1999)
26. Hall, S.R., du Boulay, D.J., Olthof-Hazekamp, R. (eds.): Xtal3.6 system. University of Western Australia, Perth (1999)
27. Sheldrick, G.M.: SADABS, empirical absorption correction program for area detector data. University of Göttingen, Germany (1996)
28. Altomare, A., Burla, M.C., Camalli, M., Cascarano, G.L., Giocavazzo, C., Guagliardi, A., Moliterni, A.G.C., Polidori, G., Spagna, S.: SIR97: a new tool for crystal structure determination and refinement. J. Appl. Crystallogr. **32**, 115–119 (1999)
29. Sheldrick, G.M.: SHELX97 programs for crystal structure analysis. University of Göttingen, Germany (1998)
30 Sheldrick, G.M.: SHELXTL-Plus Graphical interface for crystal structure solution and refinement. Bruker Analytical X-ray Instrument Inc., Maddison (1998)
31. Bruker, : Gemini: twinning solution program suite. Bruker Analytical X-Ray Instruments Inc., Madison (1999)
32. Farrugia, L.J.: WinGX suite for small-molecule single-crystal crystallography. J. Appl. Cryst. **30**, 565 (1999)